SCIENCE CHINA
Information Sciences

• RESEARCH PAPER •

August 2020, Vol. 63 182401:1–182401:7
https://doi.org/10.1007/s11432-019-2753-3

Multi-wavelength colloidal quantum dot lasers in distributed feedback cavities

Anwer HAYAT, Junhua TONG, Chao CHEN, Lianze NIU, Gohar AZIZ, Tianrui ZHAI* & Xinping ZHANG

Institute of Information Photonics Technology and College of Applied Sciences, Beijing University of Technology, Beijing 100124*, China*

Received 16 October 2019/Revised 16 December 2019/Accepted 30 December 2019/Published online 30 April 2020

Abstract Lasers with multi-wavelength colloidal quantum dots (CQDs) can be achieved using complex grating structures and flexible substrate. The structure contains graduated periods and rectangular cavity fabricated through interference lithography, which acts as the distributed feedback cavity. A layer of densely packed CQD film is deposited on the cavity via spin coating technique. The performance of CQD lasers based on different distributed feedback cavities is investigated. Multi-wavelength lasing is achieved based on a flexible rectangular cavity.

Keywords multi-wavelength, quantum dots lasers, distributed feedback, flexible, tunable

Citation Hayat A, Tong J H, Chen C, et al. Multi-wavelength colloidal quantum dot lasers in distributed feedback cavities. Sci China Inf Sci, 2020, 63(8): 182401, https://doi.org/10.1007/s11432-019-2753-3

1 Introduction

Recently, different kinds of lightemitting materials are used to advance the laser technology, including polymers and dyes [1–5]. Among them, colloidal quantum dots (CQDs) are the most promising candidate to achieve cheap and versatile optical sources because of its low-cost effective chemical manufacturing process and high photoluminescence quantum yield [6, 7]. Therefore, the properties of CQDs can be modified by using different techniques such as changing chemical compositions, surface functionalizations, sizes, and shapes [8–10]. Based on the optical quantum confinement effect and chemical composition process, CQDs have already covered the lasing wavelength in visible [11–13] and near-infrared spectral range [14]. Many efforts have been made to develop efficient CQD lasers by optimizing the gain properties of the CQDs and reducing the Auger recombination rate which limits the emission characteristics of CQD lasers [14–19]. Similarly, CQD lasers have been included in various cavities including whispering-gallery mode, vertical-cavity surface-emitting lasers, Fabry-Perot cavities, random cavities, distributed feedback (DFB) cavities and photonic crystal cavities [12, 20–27]. Among them DFB lasers have high performance, easy fabrication methods and low cost, which makes them a favorable optical technology for compact photonics and optoelectronic devices. Nowadays, multi-wavelength CQD lasers are generating a considerable interest in the field of lightbased technology because of their multi-wavelength emission in a single device. In a DFB structure, the lasing wavelength is synchronized by the Bragg's equation $2n_{\mathrm{eff}}\Lambda = m\lambda$, where n_{eff} is the effective refractive index, Λ is the grating period, λ is the lasing wavelength and m is the order of diffraction. At present, the multi-wavelength DFB lasers are achieved through adjustment of grating periods, effective refractive index, dynamic cavities, wedge shape layers, and flexible

* Corresponding author (email: trzhai@bjut.edu.cn)

© Science China Press and Springer-Verlag GmbH Germany, part of Springer Nature 2020

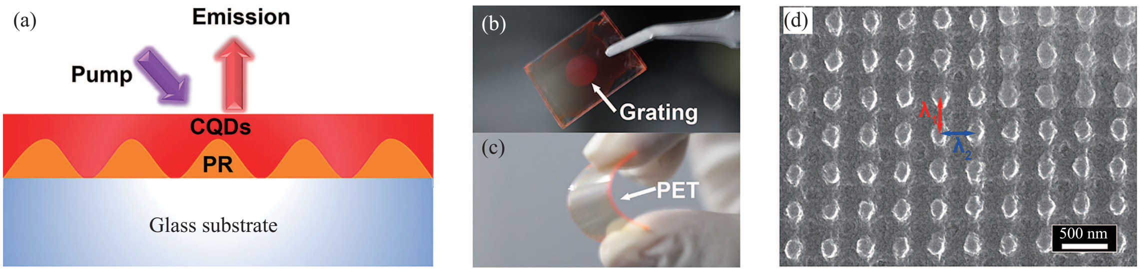

Figure 1 (Color online) (a) Schematic of the CQD laser. (b) and (c) Photographs of the flexible CQD lasers. (d) SEM image of a rectangular cavity.

materials using polymers and dyes as a gain medium [28–34]. On the other hand, multi-wavelength DFB lasers based on CQDs have not been studied systematically.

Here we report the multi-wavelength CQD DFB laser platform in which lasing wavelength changes with variation in grating periods (one and two dimensions, 1D and 2D) and from bending of soft substrate (PET). The lasing device consists of very simple structures such as photoresist (PR) grating structures and active medium. Similarly, the convenient and low-cost interference lithography is used to fabricate the grating structures for DFB lasers based on CQDs. Then the CQD is spin coated on the DFB cavity, which results into a CQD laser. A rectangular cavity CQD laser is introduced to achieve two lasing peaks in a single laser device. Multi-wavelength lasing in 1D CQD lasers is achieved through bending a flexible PET substrate.

2 Experiments

In this study, multi-wavelength CQD lasers are prepared using simple and low-cost methods, including spin coating and interference lithography. Figure 1(a) illustrates the schematic diagram of the whole 1D CQD laser device on a glass substrate. Figures 1(b) and (c) present the photograph of the fabricated 1D CQD laser platform on a flexible substrate that shows a grating structure, which will act as a DFB cavity. Similarly, the morphology of the 2D (rectangular) cavity is characterized using scanning electron microscope (SEM), as shown in Figure 1(d).

In the experiment, the photoresist (PR) is spin coated separately on glass (18 mm $\times$18 mm $\times$1 mm) and PET (18 mm $\times$ 18 mm $\times$ 0.2 mm) substrates at 2500 rpm for 30 s. Then the samples are baked on a hot plate at 110 °C (glass substrate) and 55 °C (PET substrate) for 60 s to flatten the films and evaporate the solvent. The PR films are exposed to an interference pattern of two equal laser beams each having a power of 20 mW generated by 343 nm, 1 ns and 200 Hz diode-pumped solid-state laser (FLARE NX, Coherent). The grating period Λ of DFB laser cavities can be determined by using the equation $\Lambda=0.5\lambda/\sin\theta$, where θ is the angle between two laser beams. The rectangular cavities can be fabricated through double exposures by rotating the samples 90° to the interference patterns. The exposed PR samples are developed for 6 s (glass substrate) and 13 s (PET substrate) using a developer (AR 300-47, Allresist) in order to achieve the grating structures, which will act as DFB cavities. Finally, the lightemitting CdSe/CdS/ZnS (Beijing Beida Jubang Science & Technology Co. Ltd.) core/shell/shell CQDs behaves as active materials, dissolving in a cyclohexane with a concentration of 40 mg/ml. The CQD solution is spin coated on the grating structure at 1500 rpm (glass substrate) and 1000 rpm (PET substrate) for 30 s, forming the laser device.

3 Result and discussion

Figure 2(a) presents the UV-visible absorption spectra and photoluminescence (PL) spectra of CdSe/CdS /ZnS CQD film in a cyclohexane solution at room temperature. The three peaks in the absorption spectrum (red arrows in Figure 2(a)) that correspond to the lowest exciton transition (1S (e)-1S

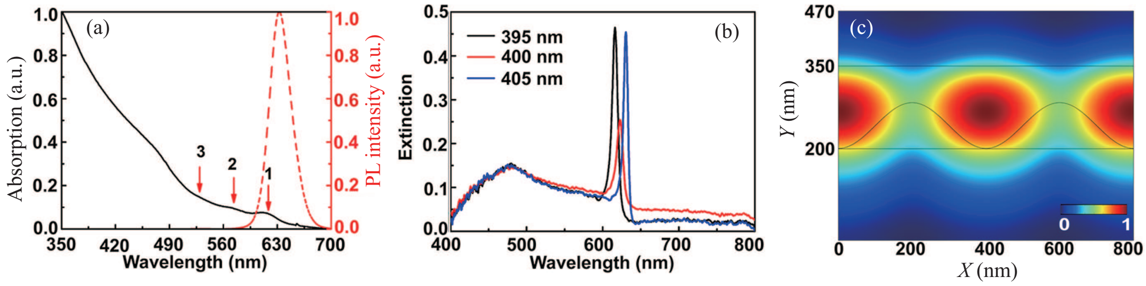

Figure 2 (Color online) Optical characterization of CQD film. (a) Absorption (black line) and PL (red line) spectra; (b) extinction spectra of 1D CQD laser with different grating periods; (c) electric field distribution of the 621 nm mode of the cavity.

3/2 (h), 1S (e)-2S 3/2 (h) and 1P (e) 1P 3/2 (h)) are well resolved [35, 36], which combine with the narrow bandwidth of the PL spectrum (FWHM$\sim$32 nm), indicating the high quality of core/shell/shell CQDs [25]. The extinction spectrum of the grating structure with three different periods having a difference of 5 nm covered with the core/shell/shell CQDs is demonstrated in Figure 2(b). The optical extinction spectrum of 1D CQD lasers samples is measured through illumination of a nonpolarized white light with a maximum power density of 0.1 mW/cm^2 from the tungsten halogen lamp (HL-200). When the CQD laser device is placed parallel to the incident light ($\theta = 0°$), two peaks are observed. The broad peaks explain the absorption spectrum of CQDs, which can also be seen in Figure 2(a). The narrow peaks are attributed to the waveguide mode of the CQD thin film. The three narrow peaks in the extinction spectra are due to the change in grating periods. The narrow peaks are red shifted in the extinction plot showing the ability of the varying grating periods to change the emission wavelength of the CQD lasers. COMSOL simulation package is employed to simulate the electric field distribution of the 621 nm mode of the CQD laser cavity, as shown in Figure 2(c). The simulator parameters are identical with the structural parameters used for 1D CQD lasers in Figure 1(a). It is confirmed from the simulation that the waveguide mode is concentrated within the CQD film. At $\lambda = 621$ nm, the effective refractive indices of the CQDs, PR and glass are 1.8, 1.51 and 1.72, respectively. All the refractive indices are measured using a spectroscopic ellipsometer (ESNano, Ellitop).

The fabricated 1D CQD lasers on the glass substrate are excited by a femtosecond laser having 400 nm wavelength, 1 kHz repetition rate, and 200 fs pulse width. A variable optical attenuator regulates the pump power. The pump beam directly impinges on the CQD laser samples without focusing on having a diameter of about 3 mm. The lasing spectra from the CQD laser platform are collected by a spectrometer (Maya 2000 Pro, Ocean Optics). Figure 3(a) shows the emission wavelength of the CQD lasers at different pump intensities. At a low pump fluence, the lasing peak is weak but when the pump fluence is above the threshold (> 20 μJ/cm^2), the lasing peak at 621 nm is observed, which is identical with the electric field distribution of the simulated waveguide mode, as shown in Figure 2(c).

Figures 3(b) and (c) illustrate the emission peaks at different pump fluences by changing the grating period with 5 nm difference. The lasing peaks are shifted toward the longer wavelength range, e.g., 628 nm and 636 nm for 400 nm and 405 nm, respectively. The linewidth of lasing peaks is about 1 nm. From Figure 3(b), it can be seen that the linewidth of the lasing peak is broadened with the increase of the input power due to the highly injected carrier density, which may change the refractive index of the materials [37]. Figure 3(d) depicts the normalized output intensity as a function of the wavelength for different grating periods. So, the laser wavelength redshifted with increasing the grating period. Figure 3(e) shows the lasing intensity as a function of the pump fluences, indicating the thresholds of 20.2 μJ/cm^2, 44.6 μJ/cm^2, and 52.6 μJ/cm^2 for 395 nm, 400 nm, and 405 nm grating periods, respectively. In Figure 3(f), the typical laser spots of different CQD DFB lasers are shown. The typical lasing spots change color with tuning emission wavelength. As noted, the laser spots look like a "cross" obtained from the combination of two arcs, with a limited width in the vertical direction, which is defined by the Bragg diffraction of the CQD DFB cavity. The fabricated 1D CQD lasers are linearly polarized. More details about the polarization effect can be found in our previous studies [38, 39]. The width (w) of the

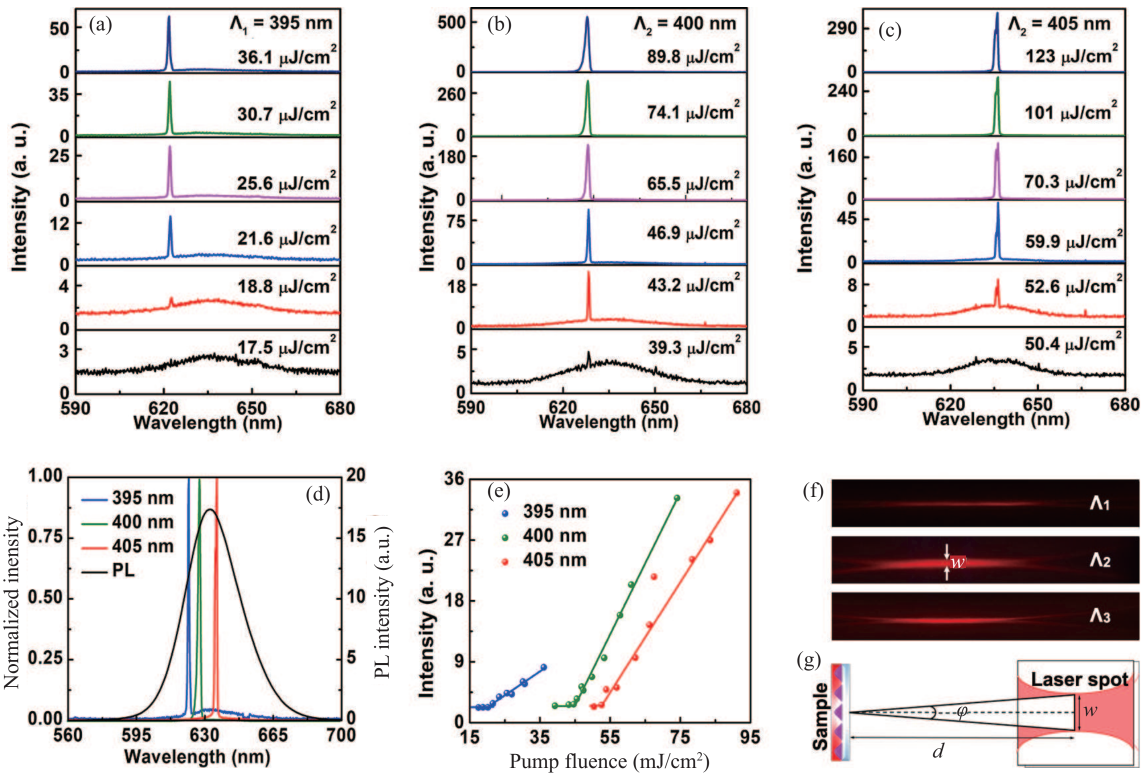

Figure 3 (Color online) Measured spectra of 1D CQD lasers with different grating periods. (a) 395 nm, (b) 400 nm, and (c) 405 nm; (d) variations of CQD laser emission wavelength with changing grating periods; (e) lasing emission intensities as function of pump fluences; (f) photographs of the laser spot of CQD lasers with different grating periods; (g) schematic diagram for measuring divergence angle.

laser spots in Figure 3(f) is 2 mm. The distance (d) between the laser spot and the sample is 100 mm. So, the divergence angle (ϕ) of the laser beam is 10 mrad.

Based on the rectangular cavity CQD DFB lasers are fabricated to achieve multi-wavelength lasing. The first systemic report on the 2D conjugated polymer DFB laser was made by Riechel et al. [40] in 2000 which achieved nearly diffraction limited surface emitting lasing. Within the framework of these criteria, three rectangular cavities are fabricated, namely, cavity 1 (402–405 nm), cavity 2 (402–408 nm) and cavity 3 (405–408 nm). The periods of the rectangular cavities are changed to study their effect on emission wavelengths, as shown in Figures 4(a)–(c). The shift in the two emission peaks for cavity 1 (λ_1 = 624 nm and λ_2 = 631 nm), cavity 2 (λ_1 = 625 nm and λ_2 = 634 nm) and cavity 3 (λ_1 = 628 nm and λ_2 = 631 nm) is observed. Interestingly, the output intensities of the 2D CQD lasers, as shown in Figures 4(a)–(c) is more efficient compared to the ID CQD lasers in Figures 3(a)–(c). As shown in Figure 4(c), with 9.9 μJ/cm^2 pump energy, the peak at the shorter wavelength shows the amplified spontaneous emission and disappears with the increase of the pump energy because of the lasing mode competition. Therefore, our experimental results are in line with the previous findings in [41], in which the feedback mechanism is more efficient for 2D DFB cavities compared to 1D DFB cavities, which leads to a lower the threshold.

The log-log threshold plots of the CQD lasers based on the rectangular cavity are presented in Figures 4(d)–(f). In there, it can be noted from the typical "S"-shaped curve of the thresholds that all the rectangular cavity lasers confirm the evolution from amplified spontaneous emission to stimulated emission for the two lasing peaks approximately at the same threshold. The output lasing spectrum from the rectangular cavity lasers can be considered as a combination of two linear polarization components (horizontal and vertical) of two 1D DFB cavities [32].

A PET soft substrate is used to modify the grating periods of 1D CQD laser device which in turn tunes the emission wavelength. Figure 5(a) demonstrates the schematic optical layout used to study the

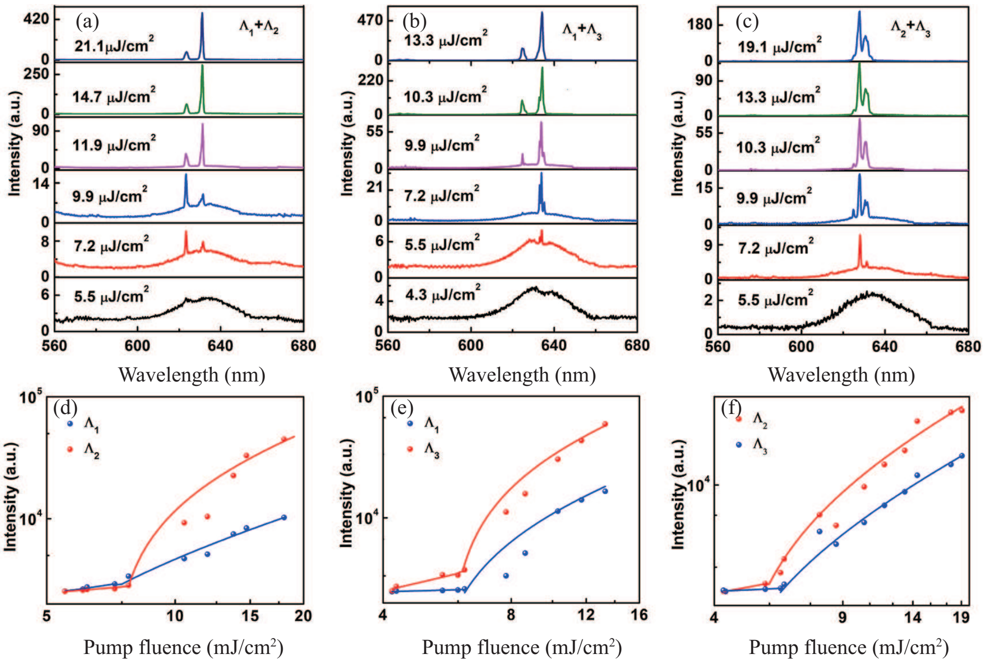

Figure 4 (Color online) Emission spectra of CQD lasers based on the rectangular cavity. (a) Cavity 1 (Λ_1 = 402 nm and Λ_2 = 405 nm); (b) cavity 2 (Λ_1 = 402 nm and Λ_3 = 408 nm); (c) cavity 3 (Λ_2 = 405 nm and Λ_3 = 408 nm); (d)–(f) thresholds (log-log plot) of the respective 2D CQD lasers.

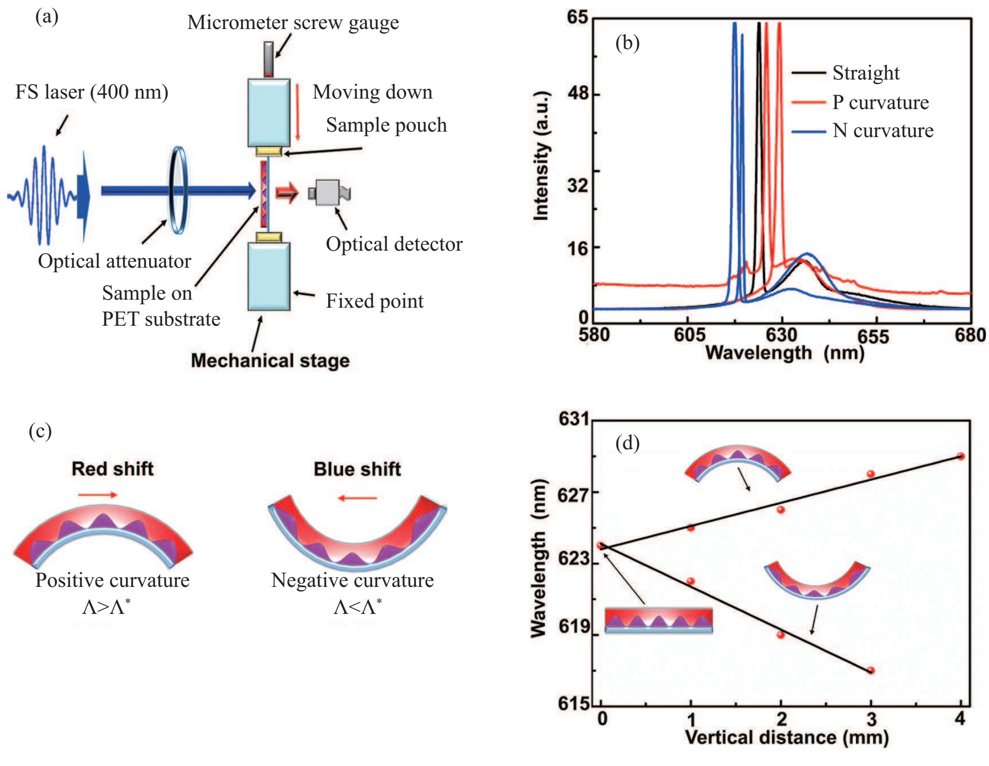

Figure 5 (Color online) (a) Schematic of CQD lasers on PET substrate; (b) measured emission spectra as a function of wavelength during bending process, without bending (black line), bend upward direction (red line), and bend downward direction (blue line); (c) bending directions; (d) emission wavelength as a function of the vertical displacement of the micrometer.

mechanical effect of PET substrate CQD laser on emission wavelengths [42].

A mechanical stage shown in Figure 5(a) contains a sample pouch in which a laser device is adjusted in a vertical direction. The pump incident perpendicular to the laser device and the output is measured on the other side using an optical spectrometer. A micrometer screw gauge is mounted on the top end of the sample pouch to bend the sample, as shown in Figure 5(a). A micrometer screw gauge is mounted on the top end of the sample pouch to move to a downward direction (shown by red line) and bend the CQD laser platform either in a positive curvature (outward direction) or a negative curvature (inward direction). Figure 5(b) demonstrates the emission wavelength above the threshold of the 1D CQD laser for different radiuses of curvature on PET substrate. When the curvature is increased positively (outward direction), the grating period ($\Lambda < \Lambda^*$) of the CQD laser on the PET substrate is slightly increased, as shown in Figure 5(c). According to Bragg's equation, the laser wavelength will be red shifted and vice versa. For these measurements, the pump energy is kept constant and the vertical distance is changed by moving the screw of the micrometer. Figure 5(d) presents the tuning of emission wavelength as a function of vertical distance changed from the micrometer screw gauge. Obviously, the laser wavelength can be tuned from 617 nm to 629 nm by simply bending the PET substrate.

4 Conclusion

In summary, the multi-wavelength CQD lasers were prepared by using the complex grating structures and from the mechanical flexibility of the PET substrate through interference lithography and spin coating technique. The laser performance for 1D and 2D cavities was investigated systematically. Furthermore, the CQD laser was transferred to the PET substrate and a mechanical tuning of laser wavelength was achieved.

Acknowledgements This work was supported by National Natural Science Foundation of China (Grant Nos. 61822501, 11574015) and Beijing Natural Science Foundation (Grant No. Z180015).

References

1 Gardner K, Aghajamali M, Vagin S, et al. Ultrabright fluorescent and lasing microspheres from a conjugated polymer. Adv Funct Mater, 2018, 28: 1802759
2 Mathies F, Brenner P, Hernandez-Sosa G, et al. Inkjet-printed perovskite distributed feedback lasers. Opt Express, 2018, 26: 144–152
3 Tsutsumi N, Hinode T. Tunable organic distributed feedback dye laser device excited through Förster mechanism. Appl Phys B, 2017, 123: 93
4 Samuel I D W, Turnbull G A. Organic semiconductor lasers. Chem Rev, 2007, 107: 1272–1295
5 Cai S S, Han Z Y, Wang F L, et al. Review on flexible photonics/electronics integrated devices and fabrication strategy. Sci China Inf Sci, 2018, 61: 060410
6 Murray C B, Kagan C R, Bawendi M G. Synthesis and characterization of monodisperse nanocrystals and close-packed nanocrystal assemblies. Annu Rev Mater Sci, 2000, 30: 545–610
7 Kagan C R, Lifshitz E, Sargent E H, et al. Building devices from colloidal quantum dots. Science, 2016, 353: 5523
8 Alivisatos A P. Semiconductor clusters, nanocrystals, and quantum dots. Science, 1996, 271: 933–937
9 Chen O, Zhao J, Chauhan V P, et al. Compact high-quality CdSe-CdS core-shell nanocrystals with narrow emission linewidths and suppressed blinking. Nat Mater, 2013, 12: 445–451
10 Guzelturk B, Kelestemur Y, Gungor K, et al. Stable and low-threshold optical gain in CdSe/CdS quantum dots: an all-colloidal frequency up-converted laser. Adv Mater, 2015, 27: 2741–2746
11 Snee P T, Chan Y, Nocera D G, et al. Whispering-gallery-mode lasing from a semiconductor nanocrystal/microsphere resonator composite. Adv Mater, 2005, 17: 1131–1136
12 Eisler H J, Sundar V C, Bawendi M G, et al. Color-selective semiconductor nanocrystal laser. Appl Phys Lett, 2002, 80: 4614–4616
13 Wang Y, Fong K E, Yang S, et al. Unraveling the ultralow threshold stimulated emission from CdZnS/ZnS quantum dot and enabling high-Q microlasers. Laser Photonics Rev, 2015, 9: 507–516
14 Heo J, Jiang Z, Xu J, et al. Coherent and directional emission at 1.55 μm from PbSe colloidal quantum dot electroluminescent device on silicon. Opt Express, 2011, 19: 26394–26398
15 Park Y S, Bae W K, Baker T, et al. Effect of auger recombination on lasing in heterostructured quantum dots with engineered core/shell interfaces. Nano Lett, 2015, 15: 7319–7328
16 Klimov V I, Ivanov S A, Nanda J, et al. Single-exciton optical gain in semiconductor nanocrystals. Nature, 2007, 447: 441–446
17 Zavelani-Rossi M, Lupo M G, Tassone F, et al. Suppression of biexciton auger recombination in CdSe/CdS Dot/Rods: role of the electronic structure in the carrier dynamics. Nano Lett, 2010, 10: 3142–3150

18 Bae W K, Padilha L A, Park Y S, et al. Controlled alloying of the core-shell interface in CdSe/CdS quantum dots for suppression of Auger recombination. ACS Nano, 2013, 7: 3411–3419

19 Grim J Q, Christodoulou S, Di Stasio F, et al. Continuous-wave biexciton lasing at room temperature using solution-processed quantum wells. Nat Nanotech, 2014, 9: 891–895

20 Wang Y, Ta V D, Leck K S, et al. Robust whispering-gallery-mode microbubble lasers from colloidal quantum dots. Nano Lett, 2017, 17: 2640–2646

21 le Feber B, Prins F, De Leo E, et al. Colloidal-quantum-dot ring lasers with active color control. Nano Lett, 2018, 18: 1028–1034

22 Rong K, Sun C, Shi K, et al. Room-temperature planar lasers based on water-dripping microplates of colloidal quantum dots. ACS Photon, 2017, 4: 1776–1784

23 Dang C, Lee J, Roh K, et al. Highly efficient, spatially coherent distributed feedback lasers from dense colloidal quantum dot films. Appl Phys Lett, 2013, 103: 171104

24 Roh K, Dang C, Lee J, et al. Surface-emitting red, green, and blue colloidal quantum dot distributed feedback lasers. Opt Express, 2014, 22: 18800–18806

25 Han C, Jung H, Lee J, et al. Wet-transfer of freestanding dense colloidal quantum dot films and their photonic device application. Adv Mater Technol, 2018, 3: 1700291

26 Wang Y, Ta V D, Gao Y, et al. Stimulated emission and lasing from CdSe/CdS/ZnS core-multi-shell quantum dots by simultaneous three-photon absorption. Adv Mater, 2014, 26: 2954–2961

27 Huang Y, Ma X, Yang Y, et al. Hybrid-cavity semiconductor lasers with a whispering-gallery cavity for controlling Q factor. Sci China Inf Sci, 2018, 61: 080401

28 Li Z, Zhang Z, Scherer A, et al. Mechanically tunable optofluidic distributed feedback dye laser. Opt Express, 2006, 14: 10494–10499

29 Stroisch M, Woggon T, Teiwes-Morin C, et al. Intermediate high index layer for laser mode tuning in organic semiconductor lasers. Opt Express, 2010, 18: 5890–5895

30 Camposeo A, Del Carro P, Persano L, et al. Electrically tunable organic distributed feedback lasers embedding nonlinear optical molecules. Adv Mater, 2012, 24: 221–225

31 Zhai T, Wang Y, Chen L, et al. Direct writing of tunable multi-wavelength polymer lasers on a flexible substrate. Nanoscale, 2015, 7: 12312–12317

32 Zhai T, Tong F, Wang Y, et al. Polymer lasers assembled by suspending membranes on a distributed feedback grating. Opt Express, 2016, 24: 22028

33 Gao Y, Huang C, Hao C, et al. Lead halide perovskite nanostructures for dynamic color display. ACS Nano, 2018, 12: 8847–8854

34 Rong K, Gan F, Shi K, et al. Configurable integration of on-chip quantum dot lasers and subwavelength plasmonic waveguides. Adv Mater, 2018, 30: 1706546

35 Klimov V I. Spectral and dynamical properties of multiexcitons in semiconductor nanocrystals. Annu Rev Phys Chem, 2007, 58: 635–673

36 Lee D U, Kim D H, Choi D H, et al. Microstructural and optical properties of CdSe/CdS/ZnS core-shell-shell quantum dots. Opt Express, 2016, 24: 350–357

37 Tang B, Dong H, Sun L, et al. Single-mode lasers based on cesium lead halide perovskite submicron spheres. ACS Nano, 2017, 11: 10681–10688

38 Chen C, Tong F, Cao F, et al. Tunable polymer lasers based on metal-dielectric hybrid cavity. Opt Express, 2018, 26: 32048

39 Cao F, Niu L, Tong J, et al. Hybrid lasing in a plasmonic cavity. Opt Express, 2018, 26: 13383–13389

40 Riechel S, Kallinger C, Lemmer U, et al. A nearly diffraction limited surface emitting conjugated polymer laser utilizing a two-dimensional photonic band structure. Appl Phys Lett, 2000, 77: 2310–2312

41 Heliotis G, Xia R, Turnbull G A, et al. Emission characteristics and performance comparison of polyfluorene lasers with one- and two-dimensional distributed feedback. Adv Funct Mater, 2004, 14: 91–97

42 Foucher C, Guilhabert B, Laurand N, et al. Wavelength-tunable colloidal quantum dot laser on ultra-thin flexible glass. Appl Phys Lett, 2014, 104: 141108